THE JOURNAL OF BIOLOGICAL CHEMISTRY VOL. 286, NO. 35, pp. 30740–30747, September 2, 2011

Sox Factors Transcriptionally Regulate *ROBO4* Gene Expression in Developing Vasculature in Zebrafish*[S]

Received for publication, January 12, 2011, and in revised form, June 13, 2011 Published, JBC Papers in Press, July 7, 2011, DOI 10.1074/jbc.M111.220665

Ganesh V. Samant[‡1], Marcus O. Schupp[‡2], Mathias François[§2], Silvia Moleri[¶], Rajendra K. Kothinti[‖], Chang Zoon Chun[‡], Indranil Sinha[‡], Suzanna Sellars[‡], Noah Leigh[‡], Kallal Pramanik[**], Mark A. Horswill[‡], Indulekha Remadevi[‡], Keguo Li[‡1], George A. Wilkinson[‡], Niloofar M. Tabatabai[‖], Monica Beltrame[¶], Peter Koopman[§], and Ramani Ramchandran[‡3]

*From the [‡]Division of Developmental Biology, Developmental Vascular Biology Program, Department of Pediatrics, Children's Research Institute, Medical College of Wisconsin, Milwaukee, Wisconsin 53226, the [§]Institute for Molecular Bioscience, the University of Queensland, Brisbane, Queensland 4072, Australia, **Prescient Life Sciences, New Delhi 122 002, India, the [¶]Dipartimento di Scienze Biomolecolari e Biotecnologie, Università degli Studi di Milano, Milan 26-20133, Italy, and the [‖]Department of Medicine and Kidney Disease Center, Medical College of Wisconsin, Milwaukee, Wisconsin 53226*

Despite their importance as members of the Roundabout (*Robo*) family in the control of axonal and vascular patterning, the transcriptional regulation of these genes is poorly understood. In this study, we show that members of the Sry-related high mobility box (Sox) transcription factor family as being transcriptional regulators of *roundabout4* (*robo4*), a *Robo* gene family member that participates in sprouting angiogenesis *in vivo*, in zebrafish. Double whole mount *in situ* hybridization analysis in zebrafish embryos revealed co-localization of the vascular relevant Sox factors *sox7* or *sox18* mRNA with *robo4* transcripts in developing intersomitic vessels. A 3-kb human *ROBO4* promoter element was able to drive reporter expression in zebrafish to recapitulate the endogenous temporal intersomitic vessel expression pattern of *robo4*. EMSA analysis confirmed binding of Sox18 to a canonical Sox binding site (from −1170 bp to −1176 bp) in the *ROBO4* promoter (3 kb), and mutation analysis indicated that this site was partially responsible for *ROBO4* promoter activity in ECs. A combination of gain- and loss-of-function analysis identified Sox7 and Sox18 co-regulation of *robo4* but not *fli1a* transcripts in zebrafish. Finally, Sox-mediated *robo4* transcriptional regulation is conserved across evolution. These studies imply Sox-mediated transcriptional regulation of *Robo4* in the developing embryonic vasculature.

In developing vertebrates, neural and vascular patterning generate intricate branching networks that share several similar features (1). However, this connectivity is governed by a limited toolkit of signaling receptor systems. These systems must therefore be subjected to exquisite control to achieve proper patterning and avoid miscues. Recently, members of the axon guidance family have shown both expression and functionality in the developing vasculature. Of the four distinct families of axon guidance signaling partners, namely Slit-Robo, Ephrin-Eph, Netrin-Unc, and Semaphorin-Plexin, our laboratory has focused on the Slit-Robo family members and their role in the vasculature.

Roundabouts (Robos),[4] a class of cell surface receptors that were originally identified to function in axon guidance (2), have recently been implicated in providing critical directional information for migration of endothelial cells (ECs) (3, 4). Four mammalian Robos are known, of which the fourth member *robo4* is expressed in the intersomitic vessels (ISVs) and is strikingly regulated with peak expression passing in a "wave" along the trunk axis from 19–29 somites (3), suggesting a high degree of transcriptional control of this gene product. Recently, a 3-kb human *ROBO4* promoter sequence has been identified that directs endothelial cell-specific expression pattern *in vivo* and *in vitro* (5). In addition, a guanine and adenine-binding protein-binding element in the *ROBO4* promoter is necessary for endothelial expression *in vivo* (6). However, to date little is known regarding transcription factors that are involved in regulating *robo4* expression during embryonic vascular development. In this study, we provide evidence for Sox7 and Sox18 transcription factors as regulators of *robo4* vascular expression during embryonic development in zebrafish. *SoxF* genes, namely *Sox7*, *Sox17*, and *Sox18*, play pivotal roles in cardiovascular development including the orchestration of endothelial cell fate and cell differentiation (7). During embryonic mouse development, *Sox7*, *Sox17*, and *Sox18* expression is evident in smaller branching vessels and ISVs (8–10) and zebrafish *sox7* and *sox18* are expressed in early angioblasts at lateral plate mesoderm and ISVs (11–13). To date, little is known in regard to transcriptional target for SoxF in the developing angiogenesis

* This work was supported, in whole or in part, by National Institutes of Health Grant HL090712 and an administrative supplement to HL090712 (to R. R.). This work was also supported by an Advancing Healthier Wisconsin grant and Children's Research Institute seed funds (to R. R.).

[S] The on-line version of this article (available at http://www.jbc.org) contains supplemental Figs. S1–S4, Methods, and additional references.

[1] Supported by American Heart Association postdoctoral awards.

[2] Both authors contributed equally to this work.

[3] To whom correspondence should be addressed: 8701 Watertown Plank Rd., Milwaukee, WI 53226. Tel.: 414-955-2387; Fax: 414-955-6325; E-mail: rramchan@mcw.edu.

[4] The abbreviations used are: Robo, human roundabout; *robo4*, zebrafish roundabout4; DA, dorsal aorta; DIG, digoxigenin; *fli*, friend leukemia virus integration; GOF, gain-of-function; hpf, hours postfertilization; ISH, *in situ* hybridization; ISV, intersomitic vessel; HUVEC, human umbilical vein endothelial cell; LOF, loss-of-function; MO, morpholino; NT, neural tube; Op, opossum; som, somite.

in vivo, and this study provides evidence that suggests *robo4* may indeed serve as one candidate.

EXPERIMENTAL PROCEDURES

Cell Culture and Zebrafish Stocks—HUVECs were purchased from Lonza and maintained in endothelial cell basal medium-2 (EBM-2; Lonza) supplemented with fetal bovine serum (FBS) (2%) and 2 units/ml gentamycin. All HUVEC experiments were performed with cells in passages 3–6. Mouse Robo4 cDNA (probe generation) and human *ROBO4* promoter-luciferase construct were kindly provided by Drs. Dean Y. Li (University of Utah) and William Aird (Beth Israel Deaconess Medical Center, Harvard). Dr. Monica Beltrame (Universita' degli Studi di Milano, Italy) provided the zebrafish *sox7* and *sox18* cDNAs. Zebrafish were grown and maintained at 28.5 °C in a 14-h day and 10-h night cycle. Mating was routinely carried out at 28.5 °C, and all embryos were staged according to established protocols. All zebrafish studies were performed under the Medical College of Wisconsin institutional guidelines (Animal Protocol 312-06-2).

RNA/MO Microinjections and in Situ Hybridization (ISH)—Zebrafish *sox7* and *sox18* RNA were transcribed by T7 polymerase from linearized vectors containing the respective inserts in pcDNA3.1. For gain-of-function (GOF) experiments, 50–75 pg of capped RNAs were injected into the embryonic cell (1-cell stage). Digoxigenin (DIG)-labeled antisense RNA probes for *fli*, and *robo4* were generated using a DIG RNA labeling kit (Roche Applied Science). The MOs used for *sox7* and *sox18* were from a previous publication (11) and were injected at a dose of 0.25 pmol/embryo. The specificity and efficacy of the MOs used in this study have been reported previously (11).

For *sox7* and *sox18*, chromogenic detection of single transcripts was carried out as described (14). For fluorogenic detection of two transcripts in co-expression studies, a DNP-labeled *robo4* probe was used together with DIG-labeled *sox7* and *sox18* probes, respectively. Hybridized probes were visualized using peroxidase conjugated anti-DIG/DNP antibodies (1:1000; Roche Applied Science), FITC- and Cy3 tyramides (1:100) from the TSA system (PerkinElmer Life Sciences) according to the manufacturer's instructions. Pictures were acquired using a Zeiss Observer Z1 inverted microscope (single staining) or a Zeiss LSM 501 confocal microscope. Confocal data were processed with AxioVision 6.8, and linear level adjustment was carried out with Adobe Photoshop CS. Details on double stainings are available upon request. The mouse probe for *Robo4* was made as described previously (15). Mouse section *in situ* hybridization was performed on 7-μm sections of paraformaldehyde-fixed, paraffin-embedded embryos. Sections were de-waxed, rehydrated, and incubated in 5 mg/ml proteinase K for 20 min at room temperature. After washing in phosphate buffered saline, sections were refixed with 4% paraformaldehyde for 10 min at room temperature, acetylated, and prehybridized with hybridization solution (50% formamide, 5× SSC, 5× Denhardt's, 250 mg/ml yeast RNA, 500 mg/ml herring sperm DNA) for 2 h at room temperature. Hybridization (hybridization solution + 0.5 μg/ml probe) was performed overnight at 60 °C. Slides were washed in 5× SSC for 5 min, 0.2× SSC for 1 h at 60 °C, 0.2× SSC for 5 min at room temperature and NT buffer (150 mM NaCl, 50 mM Tris-HCl, pH 7.5) for 5 min at room temperature, before incubating for 2 h with blocking solution (0.5% blocking powder (Roche Applied Science) in NT buffer) in a humidified chamber. Anti-DIG antibody (Roche Applied Science) at a 1:500 dilution in blocking solution was added to the slides and incubated overnight at 4 °C. Unbound antibodies were removed by washing three times in NT buffer supplemented with 0.05% Tween 40 (Sigma). Sections were equilibrated in detection buffer (0.1 M Tris, pH 8.0, 0.1 M NaCl, 10 mM $MgCl_2$) for 15 min at room temperature and incubated with color solution (BM purple; Roche Applied Science) according to the manufacturer's recommendations. Finally, sections were washed 2 × 5 min in phosphate buffered Tween and mounted in 80% glycerol in PBS. Stained sections were examined with an Olympus BX-51 microscope (DP-70 12Mp color camera).

Electrophoretic Mobility Shift Assay (EMSA)—Oligonucleotides synthesized by Integrated DNA Technologies (Coralville, IA) were used for DNA binding assays. Sequence information is provided in the supplemental Methods. Double-stranded probes were generated by heating equal molar amounts of each of the 5′→3′ oligonucleotide with its respective complementary oligonucleotide at 95 °C for 10 min followed by cooling to room temperature for 1 h. Next, double-stranded oligonucleotides were labeled with DIG-11-ddUTP using recombinant terminal transferase (20 units/ml) in a final volume of 25 μl according to the DIG Gel Shift Kit, Second Generation instructions (Roche Applied Science). EMSA was performed as we have previously described in detail (16). Briefly, DNA binding reactions were set up with 1 μg of nuclear or cytoplasmic proteins (HUVEC passage 3) and 0.08 pmol of the DIG-labeled wild-type or mutant *SOX18* probe in our modified DNA binding buffer (20 mM Hepes, pH 7.6, 10 mM $(NH_4)_2SO_4$, 0.2% Tween 20, 30 mM KCl) (17) containing 1 μg of poly(dI-dC) and 0.1 μg of poly-L-lysine in a final reaction volume of 20 μl. For supershift assays, 2–3 μl of Sox18 antibody (4 μg, EMSA certified; Santa Cruz Biotechnology) was added to the nuclear or cytoplasmic proteins prior to addition of the probe. For competition experiments, unlabeled double-stranded *SOX18* WT oligonucleotide at final concentrations of 0.08, 0.8, 4.0, 8.0, 16.0, and 32.0 pmol were added simultaneously with 0.08 pmol of DIG-labeled *SOX18* WT probe to the binding reaction with 1 μg of nuclear protein. Control reactions were performed with the probe alone. Reactions were incubated at room temperature for 15 min after which samples were subjected to electrophoresis on a 6% DNA Retardation Gel (Invitrogen). Blotting on to a positively charged nylon membrane was followed by UV cross-linking. Blots were then incubated with AP-conjugated to anti-DIG antibody followed by addition of substrate disodium 3-chloro-3-(methoxyspiro{1,2-dioxetane-3-2′-(5′-chloro)-tricyclo[3.3.3.3]decan}-4-yl) phenyl phosphate, chemiluminescent alkaline phosphatase substrate (CSPD). Fluor Chem HD from Alpha Innotech was used for chemiluminescence detection and quantification of bands was done using ImageJ software (National Institutes of Health).

Statistical Analysis—Statistical analysis was performed using the Student's *t* test with Graph Pad Prism (GraphPad Software, La Jolla, CA) and Microsoft Office Excel 2010 software package.

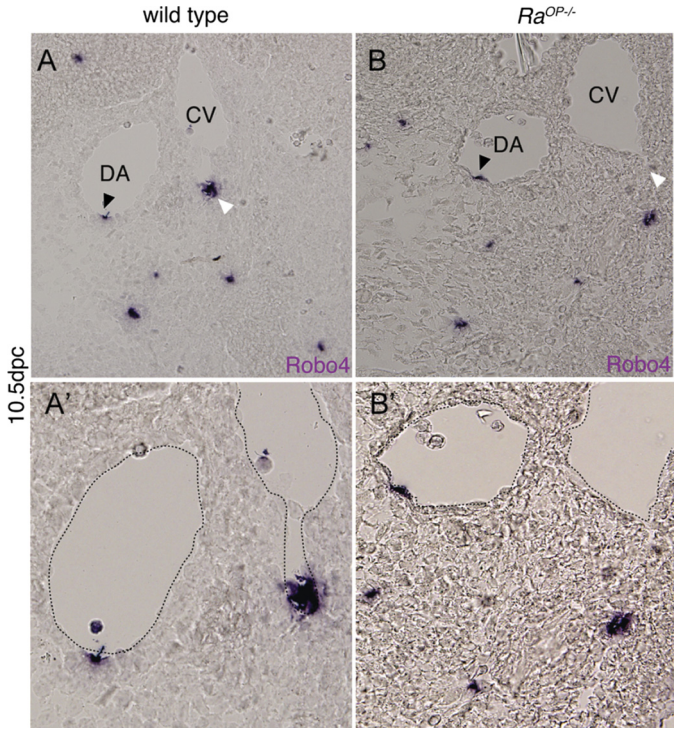

FIGURE 1. **Sox18 knock-out mice show polar loss of *Robo4* expression in caudal vein (*CV*).** *A* and *B* are transverse section of *Robo4 in situ* 10.5 days postcoitus (*dpc*) embryos (WT and $Ra^{Op-/-}$). The expression of *Robo4* is detected in the endothelium of both DA and caudal vein in dorsolateral polarized fashion. The *black arrowhead* shows *Robo4* expression in the DA, and the *white arrowhead* shows the expression in the caudal vein. *A′* and *B′* are, respectively, high power images of the *A* and *B*, respectively, with the *dotted line* outlining the DA and CV. ISH was performed on 3 WT and 3 $Ra^{Op-/-}$ homozygous embryos.

All data are presented as mean ± S.E. (*n* and *p* value are provided in each figure or legend).

RESULTS

In a microarray transcriptional profile study comparing lymphatic ECs isolated from ragged-opossum (Ra^{Op}) mutant mice ($Ra^{Op-/-}$ mice) (18, 19), which carries a mutation in Sox18 to lymphatic ECs obtained from WT mice, we observed an 8.5-fold decrease in *Robo4* transcript levels with no detectable change in *Robo1* and *Robo2* transcript levels detectable. To validate the microarray result, we performed *robo4* ISH on embryonic day 10.5 sections of $Ra^{Op-/-}$ mice and WT mice. $Ra^{Op-/-}$ mice showed diminished *robo4* expression in caudal vein ECs (Fig. 1*B*, *white arrowhead*) compared with WT mice (Fig. 1*A*). No change in *Robo4* expression was observed in dorsal aorta (DA) EC (Fig. 1*A*, *black arrowhead*), suggesting preferential venous loss of *Robo4* expression in *Sox18* KO mice. These results led us to hypothesize that Sox18 transcription factor affects transcription of *Robo4* gene during embryonic vascular development *in vivo*. To test this hypothesis, we investigated the Sox-mediated transcriptional regulation of *robo4* gene in embryonic zebrafish development.

Sox 7 and Sox 18 Transcripts Are Expressed Prior to Robo4 Transcript Expression and Co-localize during Embryonic Zebrafish ISV Development—In zebrafish, two Sox factors, namely Sox7 and Sox18, show redundant function during embryonic vascular development (11–13). We next performed whole mount ISH for *sox7* (Fig. 2, *A–F*) and *sox18* (Fig. 2, *G–L*) in zebrafish embryos ranging from 18 to 27 som compared with *robo4* between 19 and 24 som (supplemental Fig. S1, *A–C*). At 18–19 som, both *sox7* (Fig. 2*A*) and *sox18* (Fig. 2*G*, *asterisk*) expression was observed in rostral ISV sprouts as they began to emerge and in axial vessel, DA. The *robo4* expression at this time point was strong in notochord and was observed in angioblasts (supplemental Fig. S1*A*). As ISV development progresses, the expression of *sox7* (Fig. 2, *D–F*) and *sox18* (Fig. 2, *I–L*) followed a rostral-caudal temporal pattern resembling the pattern observed previously for *robo4* (3) although the *sox* expression appears a somite or two early than *robo4*. We next investigated whether *robo4*, *sox7*, and *sox18* transcripts were co-expressed in the vasculature during embryonic zebrafish development stages (19–24 som) where *robo4* is expressed in ISVs (3). Confocal analysis of two-color fluorescence ISH of the zebrafish trunk regions shows that both *sox7* (Fig. 2*P*) and *sox18* (Fig. 2*Q*) transcripts were co-localized with *robo4* transcript in the developing zebrafish vasculature. At this time point (24 hpf), *sox7* expression was noticed predominantly in the leading ISV cell (Fig. 2*P′*) whereas *sox18* expression was predominant in the axial vessels and the cell immediately ventral to the ISV leading cell (Fig. 2*Q′*). Our double ISH analysis clearly shows that both *robo4* and individual *sox* (*sox7*/*sox18*) transcripts are co-localized on ISVs. Additional inverted microscope images are provided in supplemental Fig. S2, *A–F* along with three-dimensional surface rendering of the confocal picture that capture the regions of co-localization (supplemental Fig. S2*G*). The ISV expression data together suggest that *sox7* and *sox18* are expressed in the rostral ISV sprouts prior to *robo4* and could potentially influence the highly dynamic *robo4* ISV expression observed in these stages.

Sox18 Induces ROBO4 Promoter Activity via Specific Sox Binding Site in Vitro in ECs—Because *sox7* and *sox18* were expressed prior to *robo4* during ISV development, we investigated whether Sox TFs regulated *robo4* ISVs expression level in zebrafish. To investigate this question, we utilized the 5′-flanking sequence element of the human *ROBO4* promoter, which was already shown to direct EC-specific expression *in vivo* (5, 6). Further, bioinformatic analysis of this promoter indicated the presence of putative *Sox18* TF binding consensus sequences (A/TA/TCAAA/TG) between −1170 and −1176 bp, which is conserved in mouse *Robo4* promoter between −1339 and −1405 bp as well (supplemental Fig. S1*E*). We injected the 3-kb human *ROBO4* promoter-luciferase construct alone (50 pg) or in combination with *sox18* mRNA (50 pg) at 1-cell stage into the embryonic cell and collected embryos at 18–21 som, 21–26 som, 26 som, and 24-prim6 stages for luciferase assays (Fig. 3*A*), developmental stages in which endogenous *robo4* expression is highly dynamic. Embryos from each stage were lysed and assayed for luciferase activity. Remarkably, the exogenous human *ROBO4* promoter activity drives luciferase in a pattern reminiscent of endogenous *robo4* expression in ISVs. We observed a bell-shaped curve over the time course with maximal reporter activity at around 24–26 som stage and returning to base line at 25 hpf-prim6 stage (Fig. 3*A*, *dotted line*). Interestingly, in *sox18* mRNA co-injected embryos (Fig. 3*A*, *black line*), we found that the *ROBO4* promoter activity was increased

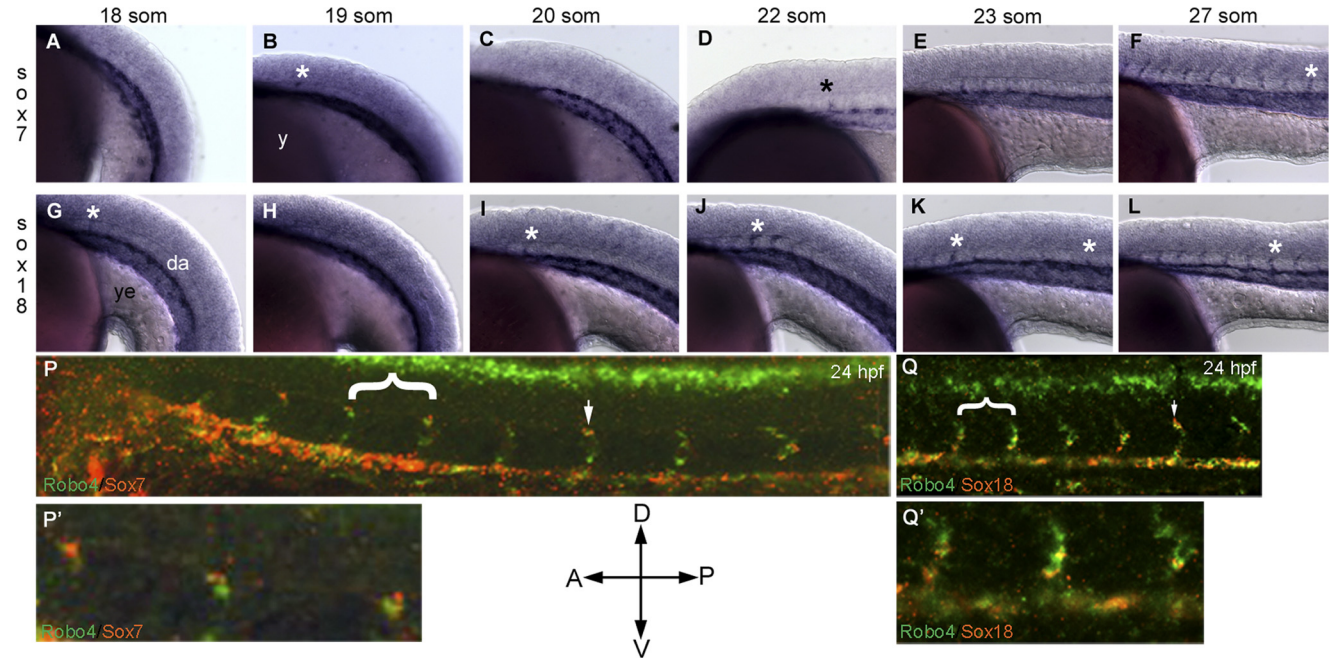

FIGURE 2. **Montage of *robo4*, *sox7*, and *sox18* endogenous expression across embryonic zebrafish development.** Whole mount for *sox7* (*A–F*), and *sox18* (*G–L*) ISH embryos were performed as indicated under "Experimental Procedures." Embryos were positioned with anterior (*A*) to the *left*, posterior (*P*) to the *right* and dorsal (*D*) to the *top* and ventral (*V*) to the *bottom* as indicated by the *orientation bars*. Embryos were staged according to the somite numbers as indicated in the respective *panels*. *Asterisks* (*black* and *white*) indicate ISVs in the zebrafish trunk region. *da*, dorsal aorta; *y*, yolk; *ye*, yolk extension. *P* and *Q* are whole mount two-color confocal fluorescent *sox7* or *sox18* (*red*) with *robo4* (*green*) ISH images of 24 hpf zebrafish trunk. *White arrows* indicate ISVs co-localized for *robo4* and *sox7*/*18* transcript. *P'* and *Q'* are higher magnification of regions highlighted by *white brackets* in *P* and *Q*, respectively.

at all time intervals compared with basal levels (Fig. 3*A*, *diamond bars*), in essence replicating the bell-shaped curve of promoter alone injected embryos but with higher luciferase values. Next, we generated four point mutants (Sox^{PM1}, Sox^{PM2}, Sox^{PM3}, Sox^{PM4}) (supplemental Fig. S1*E*) that had single nucleotide (Sox^{PM1-3}) or multiple nucleotide (Sox^{PM4}) substitutions at the putative Sox18 binding site in the *ROBO4* promoter. These constructs were individually transfected in HUVECs (Fig. 3*B*), and their activity was compared with WT human *ROBO4* promoter (supplemental Fig. S1*D*). All constructs were transfected via electroporation or Lipofectamine 2000 into HUVEC cells, and luciferase assays were performed from HUVEC lysates. Interestingly, two (Sox^{PM1} and Sox^{PM3}) of the three point mutants in addition to Sox^{PM4} showed reduction in luciferase output (Fig. 3*B*), indicating that the putative Sox binding site on −1169 bp site is responsible in part for *ROBO4* promoter activity in ECs. All groups except Sox^{PM2} were statistically significant ($p < 0.05$) compared with the WT human *ROBO4* promoter group.

To investigate whether the endogenous Sox7 or Sox18 proteins are responsible for the *ROBO4* promoter activity observed in human ECs, we utilized *sox7* or *sox18* gene-specific efficacy-confirmed siRNAs (Santa Cruz Biotechnology) (supplemental Fig. S2*I*) to knock down endogenous Sox proteins and measured luciferase activity output of the h*ROBO4* promoter. The luciferase activity is greatly reduced from the *ROBO4* promoter co-transfected with *Sox7*/*18* double siRNA sample compared with *ROBO4* promoter-luciferase construct alone (Fig. 3*C*, $p < 0.05$). To determine conclusively whether Sox7/18 proteins bind to putative Sox binding site in *ROBO4* promoter, we performed an EMSA (Fig. 3*D*) with nuclear extracts from ECs using a WT *ROBO4* promoter oligonucleotide probe and Sox18 mutant *ROBO4* promoter oligonucleotide probes (M1 and M2). As observed in the EMSA blot, the nuclear proteins from HUVECs in the WT probe lane clearly formed two complexes: complex 1 (slower migrating) and complex 2 (faster migrating) band (Fig. 3*D*). Interestingly, the M1 mutant *ROBO4* promoter oligonucleotide probe also showed the presence of the two complexes albeit of lower intensity (Fig. 3*D*, *M1 lane*). Because the M1 mutant probe has additional Sox18 binding sites, which likely serves as alternate site for interaction, we generated a second mutant probe M2, where we mutated this site (for mutant probe sequences, see supplemental Methods). Clearly, the M2 probe shows lower intensities in complex 2 (Fig. 3*D*, *M2 lane*). When the complex intensities in M1 and M2 probe lanes for nuclear protein extracts (*N*) were compared across three independent experiments with WT probe bands, we noticed a 70 and 90% decrease in complex 1 (M1: *, $p < 0.001$; M2: **, $p < 0.0005$), and a 50 and 70% decrease in complex 2 (M1: #, $p < 0.001$; M2: ##, $p < 0.005$) for M1 and M2 probes (Fig. 3*E*). The M2 probe showed lower intensities for both complexes compared with the M1 probe. Both complexes also showed a dose-dependent reduction in intensity when unlabeled competitor probes was included in the EMSA reaction (supplemental Fig. S3*B*).

To determine whether *SOX18* protein was present in the shifted complexes, we performed supershift assays with *SOX18* antibody (Fig. 3*D*, *Ab lane*). Supershift results indicated the presence of *SOX18* in both complex 1 (*black arrow*), and 2 (*gray arrow*) (Fig. 3*D*, *lanes N* and *Ab*). In addition, when binding reactions with the mutant (M1, data not shown) and WT probes (Fig. 3*D*, lane +*SOX18 Ab*) were performed in the pres-

ence of *SOX18* antibody, the complex 1 band completely disappeared in WT probe lane (data not shown for M1), and the intensity of the complex 2 band decreased by 49 and 65% in reactions with M1 and WT probes, respectively. Collectively, these data suggest that Sox18 is part of the complex that binds to *ROBO4* promoter sequences and, in addition other co-factors may also be responsible in part for *ROBO4* promoter activity in ECs.

Taking the *in vivo* human *ROBO4* promoter activity across ISV development, the ability of Sox18 to induce the *ROBO4* promoter robustly *in vivo*, point mutation analysis and Sox siRNA experiments *in vitro*, and the EMSA analysis data

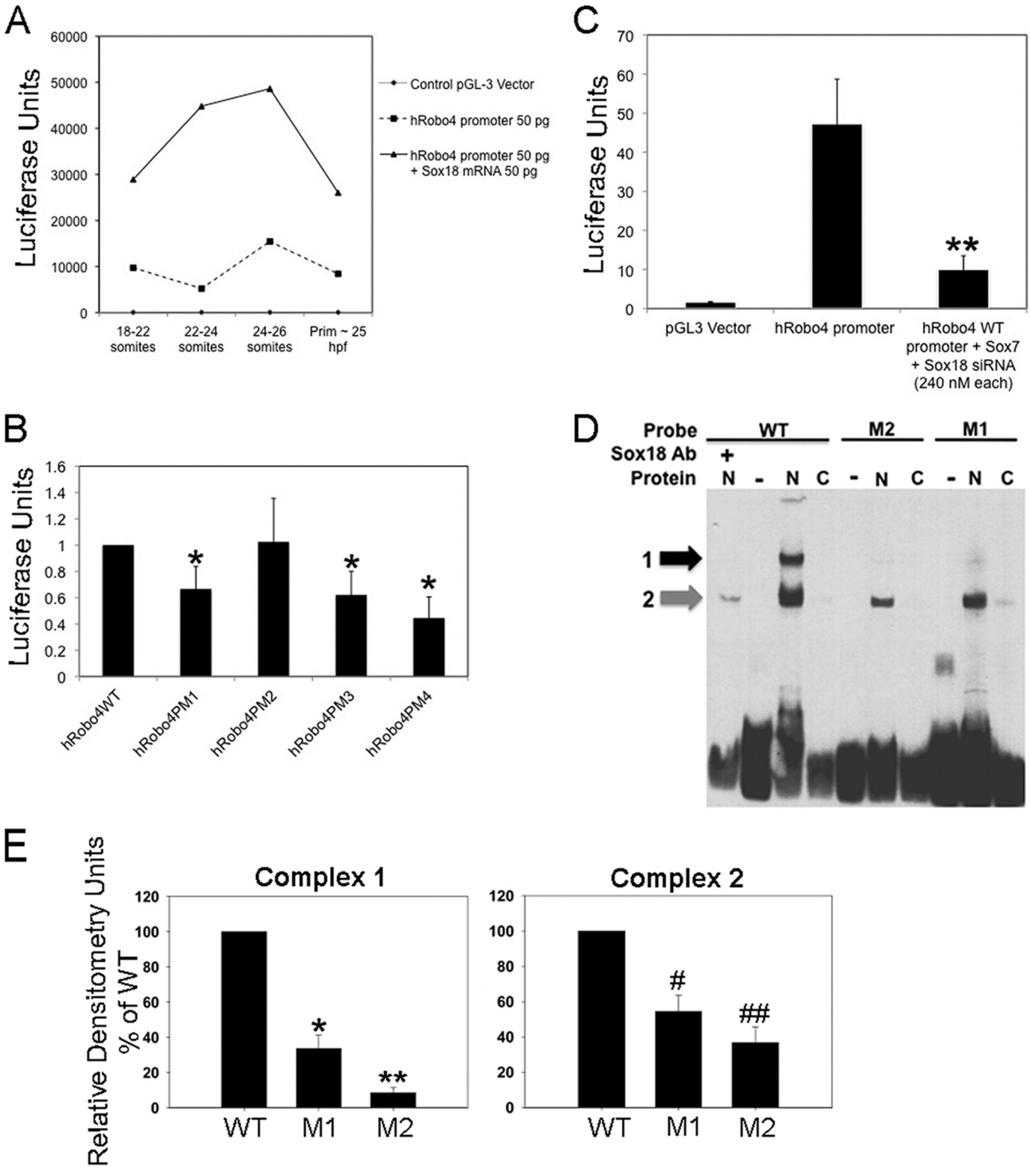

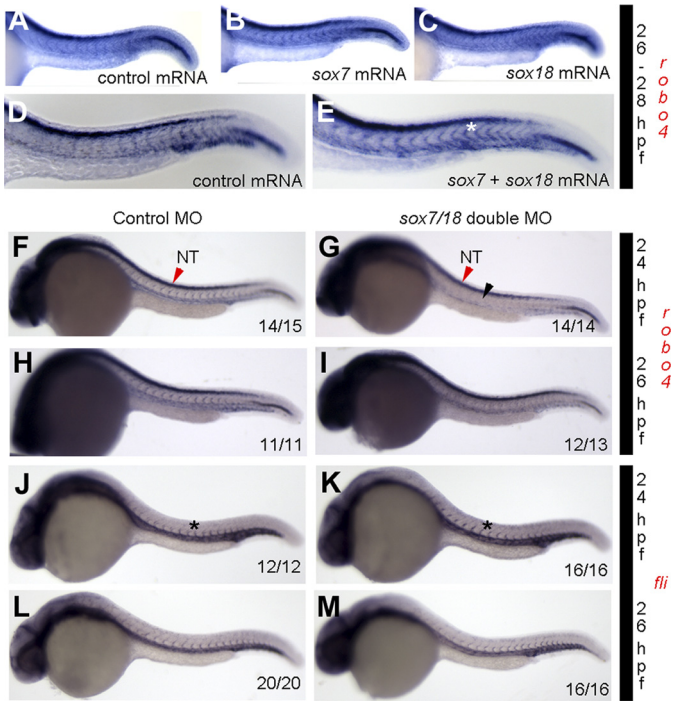

FIGURE 4. **Sox GOF and LOF show reciprocal change in *robo4* transcript expression but no changes in *fli* expression.** *A–E*, *robo4* ISH trunk expression between 26 and 28 hpf zebrafish embryo microinjected with control (*A* and *D*), *sox7* (*B*), *sox18* (*C*), and *sox7* + *sox18* mRNA (*E*) (50 pg each). *A–E* show strong *robo4* expression in the neural tube. However, *sox7* + *sox18* double mRNA injected embryos show strong *robo4* expression in the ISV (*asterisk*). Experiments were repeated three independent times, and *pictures* are representative of 15 embryos/injection group. Additional quantification is provided in supplemental Fig S2*F*. *F–M*, *robo4* ISH trunk expression in 24 hpf (*F* and *G*) and 26 hpf (*H* and *I*) and *flia* at 24 hpf (*J* and *K*) and 26 hpf (*L* and *M*) zebrafish embryos injected with control MO (*F*, *H*, *J*, and *L*) and *sox7* + *sox18* double MO (*G*, *I*, *K*, and *M*). The *inset numbers* in *F*, *G*, *H*, *I*, *J*, *K*, *L*, and *M* indicate number of embryos that show phenotype similar to that in the *image*. *Asterisks* in *J* and *K* and *black arrowhead* in *G* indicate ISV expression. *Red arrowheads* in *F* and *G* indicate NT *robo4* expression.

together we conclude that Sox7/18 are responsible in part for inducing *ROBO4* promoter activity in ECs *in vivo* and *in vitro*.

Sox GOF or LOF Embryos Show Complementary Gain or Loss of robo4 Expression—To investigate whether endogenous *robo4* expression is modulated by Sox transcription factors, we performed GOF and LOF for *sox7* and *sox18* in zebrafish embryos. For GOF experiments, we injected *sox7* or *sox18* mRNA alone or in combination into 1-cell embryo and checked *robo4* expression by ISH at 26–28 hpf. The *robo4* ISV expression is enhanced in *sox7* + *sox18* mRNA (Fig. 4*E*, *white asterisk*)-injected embryos compared with *sox7* (Fig. 4*B*) or *sox18* (Fig. 4*C*) or control mRNA (Fig. 4*D*) alone injected embryos at 24 hpf, which suggests co-operative interaction between the two factors in inducing *robo4* ISV expression. Conversely, in LOF experiments, double knockdown of *sox18*/*sox7* using MOs resulted in a diminished *robo4* expression at 24 hpf (Fig. 4*G*) and 26 hpf (Fig. 4*I*) compared with control MO (Fig. 4, *F* and H) injected embryos. At 24 hpf, 40 of 42 (95%) *sox18*/*sox7* double knockdown embryos show the phenotype depicted in Fig. 4*G*. At 26 hpf, 26 of 27 double morphants showed diminished *robo4* expression (Fig. 4*I*). Interestingly, the diminished expression was selectively observed in the ISVs (Fig. 4*G*, *black arrowhead*) with little to no qualitative change detected in the neural tube (Fig. 4, *G* and *F*, *NT*, *red arrowhead*). We also checked *fli1a* expression in control MO (Fig. 4, *J* and *L*) and *sox7*/*18* double MO injected (Fig. 4, *K* and *M*) 24 or 26 hpf embryos and observed no change (Figs. 4, *J* and *K*, *black asterisk*) in control (21 embryos) and double morphants (32 embryos), suggesting specificity of Sox regulation of *robo4* ISV expression. Further, quantitative PCR for *robo4* and *robo1* transcripts in Sox knockdown embryos shows selective down-regulation of *robo4 versus robo1* transcripts (supplemental Fig. S3*C*). This also suggests some level of Robo specificity for Sox-mediated transcriptional regulation during development.

Because *robo4* expression is also observed prior to 24 hpf in nonvascular tissues such as neural tube (NT) and notochord, we investigated the effect of *sox7* or *sox18* or double (*sox7* + *sox18*) mRNA-injected embryos for *robo4* transcript expression at 18 hpf (supplemental Fig. S4). At 18 hpf, little to no change was observed in *robo4* expression in notochord. However, in NT (supplemental Fig. S4, *B–D, black asterisk*) and midbrain-hindbrain boundary (supplemental Fig. S4, *B–D, red arrow*), we observed an expansion in the *robo4* expression domain in *sox7* (supplemental Fig. S4*B*) or *sox18* (supplemental Fig. S4*C*) or *sox7* + *sox18* (supplemental Fig. S4*D*) mRNA-injected embryos. Quantitation shows >60% of injected embryos show strong overall *robo4* induction qualitatively in midbrain-hindbrain boundary and NT (supplemental Fig. S4*E*) at 18 hpf. This result is not totally unexpected because Sox proteins are well known to function in neural development (20, 21). At 24 hpf, quantitation was performed for *robo4* induction in ISVs (supplemental Fig. S4*F*). The Sox GOF and LOF

FIGURE 3. **Robo4:Sox7/18 transcriptional regulation.** *A*, graphical representation of Sox18-induced *ROBO4* promoter activity *in vivo*. Details of the experimental design are provided under "Experimental Procedures." *Dotted line* denotes the base-line exogenous *ROBO4* promoter activity. *Black line* denotes exogenous *ROBO4* promoter activity in *sox18* overexpression (*sox18* mRNA) embryos. *Line* along the *x* axis indicates empty control pGL3 vector-injected embryos. The graph is a representative experimental data set, and each time interval contained 20–25 embryos. This experiment was performed twice with identical trends, and *error bars* have not been provided due to the high variation in the luciferase values from one experiment to the next. *B*, *in vitro* luciferase assays in HUVECs for *ROBO4* promoter point mutants (PM1–4) compared with h *ROBO4* WT promoter. *Error bars* represent S.E. from three independent experiments, and all luciferase values are shown as -fold compared with h *ROBO4* WT promoter sample. All sample groups were compared with h *ROBO4* WT promoter groups, and all samples except h *ROBO4*PM2 were statistically significant at $*p < 0.05$. *C*, *ROBO4* promoter activity in control (*lacZ* siRNA) and *Sox7* and *Sox18* knockdown (*Sox7* + *Sox18* siRNA) ECs. *B* and *C*, HUVECs transiently transfected with WT-Robo4 and Robo-4 $^{PM1-4}$ (four mutants) constructs or WT h *ROBO4* promoter (1.5 μg) and lacZ and *Sox7* + *Sox18* siRNA (240 nM each) for 36 h and promoter activity determined as a function of luciferase activity. Luciferase (firefly) readings were normalized to the control, and data from three independent experiments are compiled together. $**, p < 0.05$ was determined by two-tailed statistical analysis. *D*, EMSA of DNA binding reactions with Sox18 mutant (M1 and M2) and WT probes incubated with nuclear (*N*) or cytoplasmic (*C*) proteins from ECs, in the presence or absence of *SOX18* antibody (*Ab*). The *black* and *gray arrows* indicate the shifted complex 1 and 2, respectively. Complex 1, *top band* (*black arrow*), is diminished in intensity in mutant M1 probe *N* lanes and is absent in mutant M2 probe and wild-type probe plus Ab lanes. *E*, chemiluminescence values of the complex 1 and 2 bands (arbitrary unit) measured by Fluor Chem HD and band intensities of the two complexes in M1 and M2 probe EMSA relative to WT probe EMSA. Data are from three independent EMSA reactions, and *error bars* represent S.E. (Complex 1 M1: $*, p = 0.0009$; M2: $**, p = 0.0001$; Complex 2 M1: #, $p = 0.0076$; M2: ##, $p < 0.0018$).

results when taken together show complementary changes in *robo4* ISV expression *in vivo*, which is in agreement with the redundant function of Sox7 and Sox18 function in zebrafish vascular development (11). Taking the mouse data together from Fig. 1, these data also suggest that Sox-mediated transcriptional regulation of *Robo4* is conserved across evolution.

DISCUSSION

This study identifies members of the Sox protein transcription factor family as putative regulators of *Robo4* gene expression *in vivo*. The primary findings of this study include the following: (i) early temporal expression of *sox7* and *sox18* transcripts in DA prior to *robo4* expression; (ii) remarkably conserved human *ROBO4* promoter activity in its behavior in zebrafish, correlating well with vascular *robo4* expression pattern *in vivo*; (iii) polar regulation of *robo4* expression via Sox in zebrafish and mice; (iv) Sox7 and Sox18 along with temporal and spatial specific co-factors in regulation of *robo4* transcript expression in the vasculature.

Whole mount ISH for *sox7* and *sox18* during zebrafish ISV development shows a preponderance of *sox7* transcript in the tip of the leading sprout and *sox18* transcript in the base of the sprout with prominent expression in axial vessels. Further, both *sox7* and *sox18* transcripts appear in the rostral sprouts earlier than *robo4* expression, suggesting regulatory mechanisms of Sox and Robo in ISV sprouting process. In terms of *robo4*, ISV expression is tightly controlled across a short temporal window, and the expression is observed along the length of the entire sprout as well as the DA. These data argue that different Robo-Sox combinations are involved in ISV cell development *in vivo*. Perhaps Robo4 and Sox7 in the tip and Robo4 and Sox18 in the base of the sprout function together to direct and maintain ISV sprout formation. Whether the expression levels of *sox* transcripts correlate with protein expression and function is not known. Interestingly, the polar distribution of *sox* transcripts in zebrafish ISVs suggests polar regulation of *robo4* transcript, which is curiously observed in mice. The *Robo4* expression in Ra^{Op} mutant mice is selectively down-regulated in vein but not in artery, suggesting selective regulatory function of Sox-mediated *Robo4* induction in vein. It is worthwhile to note that the site of *Robo4* expression in vein is the area where emergence of Sox18-mediated lymphatic $Prox1^{+}$ cells is noted (22), postulating a role of Robo4 in lymphatic ECs cell directional sprouting. Because lymphatic ECs derive from venous ECs (23) it is tempting to speculate that the selective regulation of Sox-mediated *Robo4* induction in venous ECs is potentially the event that triggers the directional migration of *Prox1* LECs from vein.

In terms of evolution, both mouse and human *ROBO4* promoter share a Sox18 binding site proximal to the start site (−1170 in human and −1339 in mouse). Because *robo4* ISV expression is dynamically controlled across a short temporal window (18–29 hpf), this would suggest tight control of *ROBO4* promoter activity during this time frame. In fact, a previously published 3-kb human *ROBO4* promoter (5, 6) that shows endothelial-restricted expression in mice behaves similarly in zebrafish across the short temporal window of *robo4* ISV expression. This remarkable correlative behavior is enhanced when exogenous *sox18* mRNA is provided and is diminished when the Sox18 binding site is mutated. Although the *ROBO4* promoter activity is not lost completely in the absence of Sox18 binding site, which is expected because other sites on the promoter such as guanine and adenine-binding protein-binding element has also been shown previously to be necessary for endothelial expression *in vivo* (6). In fact, at least three pieces of distinct experimental evidence point to the role of co-factors that participate with Sox in regulating *robo4* ISV expression. (i) Mutation of Sox binding site on *ROBO4* promoter (Fig. 3*B*) does not result in complete loss of *ROBO4* promoter activity in ECs. (ii) The EMSA study shows that Sox18 mutant probe (M1) clearly binds to non-Sox nuclear proteins, which is not blocked by Sox18 antibody (data not shown). (iii) Sox GOF single mRNA and double mRNA-injected embryos (Fig. 4, *A–D*) show differential *robo4* transcript regulation at 18 hpf (individual Soxs and double Soxs) (supplemental Fig. S4) and 24 hpf (only double Soxs) (Fig. 4) presumably mediated by different sets of co-factors expressed at these time points during embryonic development. The 24 hpf double mRNA data are in agreement with redundant function of Soxs in vascular development in zebrafish (11).

In this study, we provide convincing data in three species, each of which independently provides evidence that Sox transcription factors putatively regulate *robo4* gene expression. In each of these systems there is ample published evidence of conservation of the molecular mechanisms of vascular development for *Sox* and *Robo* (3, 7, 9, 11, 13, 15, 18, 24). In addition, the genes investigated in our study are well conserved at the sequence level between the species. In sum, the presented zebrafish, mouse, and human EC data make a substantive body of evidence for conservation of this observation in development. This study for the first time provides a molecular link between Sox and Robo family in vascular development, a paradigm recently shared by another axon guidance gene of the ephrin-Eph family (25).

Acknowledgments—We thank members of the Vascular Biology Affinity Group and the Developmental Biology Group for invaluable input in these studies. We are grateful to Marc Achen, Steven Stacker, and Tara Karnezis for generously providing unpublished microarray data on the transcriptional profile study comparing lymphatic ECs from Sox18 KO and WT mice. We thank Suresh Kumar of the Medical College of Wisconsin/Children's Research Institute confocal facility with assistance in obtaining zebrafish trunk ISV images.

REFERENCES

1. Carmeliet, P., and Tessier-Lavigne, M. (2005) *Nature* **436,** 193–200
2. Kidd, T., Brose, K., Mitchell, K. J., Fetter, R. D., Tessier-Lavigne, M., Goodman, C. S., and Tear, G. (1998) *Cell* **92,** 205–215
3. Bedell, V. M., Yeo, S. Y., Park, K. W., Chung, J., Seth, P., Shivalingappa, V., Zhao, J., Obara, T., Sukhatme, V. P., Drummond, I. A., Li, D. Y., and Ramchandran, R. (2005) *Proc. Natl. Acad. Sci. U.S.A.* **102,** 6373–6378
4. Kaur, S., Castellone, M. D., Bedell, V. M., Konar, M., Gutkind, J. S., and Ramchandran, R. (2006) *J. Biol. Chem.* **281,** 11347–11356
5. Okada, Y., Yano, K., Jin, E., Funahashi, N., Kitayama, M., Doi, T., Spokes, K., Beeler, D. L., Shih, S. C., Okada, H., Danilov, T. A., Maynard, E., Minami, T., Oettgen, P., and Aird, W. C. (2007) *Circ. Res.* **100,** 1712–1722
6. Okada, Y., Jin, E., Nikolova-Krstevski, V., Yano, K., Liu, J., Beeler, D.,

Spokes, K., Kitayama, M., Funahashi, N., Doi, T., Janes, L., Minami, T., Oettgen, P., and Aird, W. C. (2008) *Blood* **112,** 2336–2339
7. Francois, M., Koopman, P., and Beltrame, M. (2010) *Int. J. Biochem. Cell Biol.* **42,** 445–448
8. Pennisi, D., Bowles, J., Nagy, A., Muscat, G., and Koopman, P. (2000) *Mol. Cell. Biol.* **20,** 9331–9336
9. Sakamoto, Y., Hara, K., Kanai-Azuma, M., Matsui, T., Miura, Y., Tsunekawa, N., Kurohmaru, M., Saijoh, Y., Koopman, P., and Kanai, Y. (2007) *Biochem. Biophys. Res. Commun.* **360,** 539–544
10. Young, N., Hahn, C. N., Poh, A., Dong, C., Wilhelm, D., Olsson, J., Muscat, G. E., Parsons, P., Gamble, J. R., and Koopman, P. (2006) *J. Natl. Cancer Inst.* **98,** 1060–1067
11. Cermenati, S., Moleri, S., Cimbro, S., Corti, P., Del Giacco, L., Amodeo, R., Dejana, E., Koopman, P., Cotelli, F., and Beltrame, M. (2008) *Blood* **111,** 2657–2666
12. Herpers, R., van de Kamp, E., Duckers, H. J., and Schulte-Merker, S. (2008) *Circ. Res.* **102,** 12–15
13. Pendeville, H., Winandy, M., Manfroid, I., Nivelles, O., Motte, P., Pasque, V., Peers, B., Struman, I., Martial, J. A., and Voz, M. L. (2008) *Dev. Biol.* **317,** 405–416
14. Oxtoby, E., and Jowett, T. (1993) *Nucleic Acids Res.* **21,** 1087–1095
15. Park, K. W., Morrison, C. M., Sorensen, L. K., Jones, C. A., Rao, Y., Chien, C. B., Wu, J. Y., Urness, L. D., and Li, D. Y. (2003) *Dev. Biol.* **261,** 251–267
16. Tabatabai, N. M., Blumenthal, S. S., and Petering, D. H. (2005) *Toxicology* **207,** 369–382
17. Kothinti, R. K., Blodgett, A. B., Petering, D. H., and Tabatabai, N. M. (2010) *Toxicol. Appl. Pharmacol.* **244,** 254–262
18. François, M., Caprini, A., Hosking, B., Orsenigo, F., Wilhelm, D., Browne, C., Paavonen, K., Karnezis, T., Shayan, R., Downes, M., Davidson, T., Tutt, D., Cheah, K. S., Stacker, S. A., Muscat, G. E., Achen, M. G., Dejana, E., and Koopman, P. (2008) *Nature* **456,** 643–647
19. James, K., Hosking, B., Gardner, J., Muscat, G. E., and Koopman, P. (2003) *Genesis* **36,** 1–6
20. Cheung, M., and Briscoe, J. (2003) *Development* **130,** 5681–5693
21. Honoré, S. M., Aybar, M. J., and Mayor, R. (2003) *Dev. Biol.* **260,** 79–96
22. Srinivasan, R. S., Geng, X., Yang, Y., Wang, Y., Mukatira, S., Studer, M., Porto, M. P., Lagutin, O., and Oliver, G. (2010) *Genes Dev.* **24,** 696–707
23. Srinivasan, R. S., Dillard, M. E., Lagutin, O. V., Lin, F. J., Tsai, S., Tsai, M. J., Samokhvalov, I. M., and Oliver, G. (2007) *Genes Dev.* **21,** 2422–2432
24. Pennisi, D., Gardner, J., Chambers, D., Hosking, B., Peters, J., Muscat, G., Abbott, C., and Koopman, P. (2000) *Nat. Genet.* **24,** 434–437
25. Parrinello, S., Napoli, I., Ribeiro, S., Digby, P. W., Fedorova, M., Parkinson, D. B., Doddrell, R. D., Nakayama, M., Adams, R. H., and Lloyd, A. C. (2010) *Cell* **143,** 145–155